

Generation of 0.1-TW optical pulses with a single-stage Ti:sapphire amplifier at a 1-kHz repetition rate

M. Hentschel¹, Z. Cheng², F. Krausz¹, Ch. Spielmann¹

¹Institut für Photonik, Technische Universität Wien, Gusshausstrasse 27/387, 1040 Wien, Austria

(Fax: +43-1/58801-38799, E-mail: michael.hentschel@tuwien.ac.at)

²Femtolasers GmbH

Received: 1 October 1999/Revised version: 16 March 2000/Published online: 24 May 2000 – © Springer-Verlag 2000

Abstract. We present a kHz-rate all-solid-state Ti:sapphire oscillator–amplifier system producing 1.8 mJ sub-20 fs pulses using a single multipass amplifier stage pumped by ≈ 10 mJ pulses. Compensation for gain narrowing and high-order dispersion is provided by chirped dielectric multilayer optics. The focused peak intensity approaches 10^{18} W/cm², making this compact high-repetition-rate source attractive for a wide range of high-field applications.

PACS: 42.60.Da; 42.60.Jf; 42.60.LH

Titanium:sapphire-based oscillator–amplifier systems drawing on the concept of chirped pulse amplification have become the standard tabletop sources of high-intensity optical pulses in the last few years. At repetition rates of 10–50 Hz, the generation of pulses with multiterawatt peak power has been demonstrated [1]. More recently, amplifiers delivering pulses with peak powers beyond 0.1 TW at a 1 kHz repetition rate have also been reported [2–6]. All these systems consist of grating stretcher–compressor arrangements and several amplifier stages pumped by several Q-switched lasers, resulting in a high degree of complexity and occupying large amounts of space. In this paper we present, for what is to our knowledge the first time, a kHz laser generating 0.1 TW pulses by using a single amplifier stage and a single Q-switched pump source. Owing to a stretcher–compressor technique that obviates the need for lossy diffraction gratings [7], as much as 17% of the pump pulse energy is converted into recompressed output pulse energy. To explore the potential of this efficient and compact system for high-field applications, we have thoroughly characterized the output temporally, spectrally and spatially.

1 Modeling of the amplification process

1.1 Gain narrowing

Due to the finite fluorescence bandwidth of Ti:sapphire and the huge factor of amplification, the spectral width of the input

pulses is decreased by a considerable amount. To estimate the required compensation, we used a simple model for the gain-narrowing process. Making use of the atomic gain coefficient

$$\alpha(\omega) = \frac{\sigma N}{1 + [2(\omega - \omega_a)/\Delta\omega_a]^2}, \quad (1)$$

one can express the power gain as

$$G(\omega) = \exp[\alpha(\omega)L] \quad (2)$$

$$= \exp\left[\frac{\sigma NL}{1 + [2(\omega - \omega_a)/\Delta\omega_a]^2}\right], \quad (3)$$

where σ is the emission cross-section (3×10^{-19} cm² for Ti:sapphire [8]), N is the population inversion, ω_a is the atomic transition frequency, $\Delta\omega_a$ is the atomic linewidth and L is the total pathlength in the crystal [9]. The impact of this frequency-dependent power gain on a measured oscillator spectrum is shown in Fig. 1 for a net power gain of 10^6 . The spectral width is reduced from 148 nm to 41 nm full width at half maximum (FWHM).

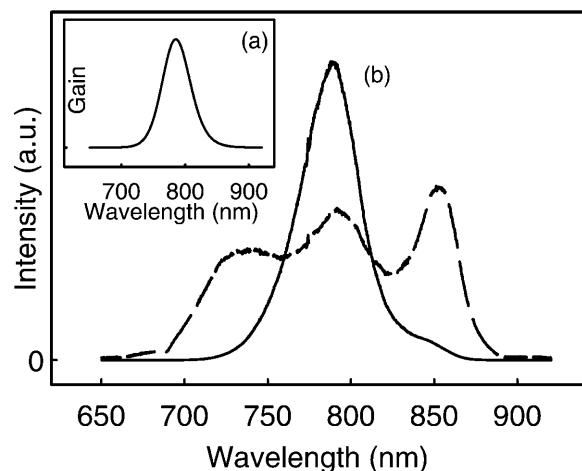


Fig. 1. **a** Power gain. **b** Measured input spectrum (*dashed*) and calculated amplified spectrum (*solid*)

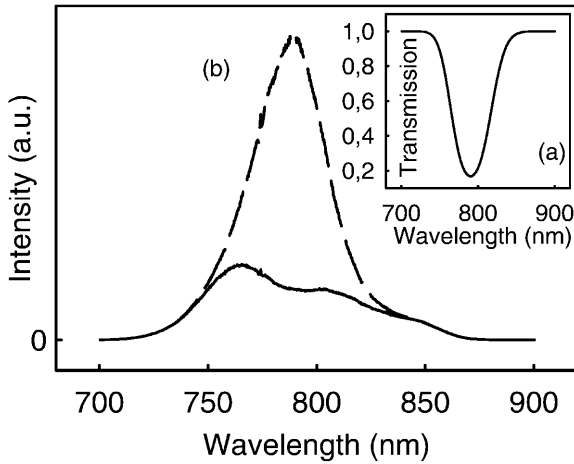


Fig. 2. **a** Filter transmission. **b** Calculated amplified spectrum with (*solid*) and without (*dashed*) filters

Using a spectral amplitude filter (Fig. 2a) one can partly compensate for gain narrowing. The spectral width is increased from 41 nm to 75 nm (Fig. 2b).

1.2 Gain saturation

As long as the population inversion is not substantially depleted, the amplification factor does not depend on the energy of the seed pulses (linear regime). In this case the so called small-signal gain is given by

$$G_{\text{lin}} = \exp(\sigma NL), \quad (4)$$

where σ is the emission cross-section, N is the population inversion, and L the length of the amplifier medium.

When the inversion is significantly reduced by the amplification process, the amplifier enters the saturated regime where the gain decreases with rising input-pulse energy. In this mode of operation the gain can be written as

$$G_{\text{sat}} = \frac{E_{\text{out}}}{E_{\text{in}}} = G_{\text{lin}} \exp\left(-\frac{E_{\text{out}} - E_{\text{in}}}{F_{\text{sat}} A}\right), \quad (5)$$

with the saturation fluence $F_{\text{sat}} = \hbar\omega/\sigma$ and the illuminated area A .

Operating an amplifier close to saturation allows the optimization of the energy extraction on the one hand and makes the output energy less susceptible to fluctuations of pump and seed pulses on the other hand. As the stored energy is removed by the traversing seed pulse, the leading edge will always undergo a stronger amplification than the trailing edge. This amplitude-shaping effect shifts the center of gravity of the pulse envelope forward in time, and in case of chirped pulse amplification the pulse spectrum experiences a redshift, assuming a positive chirp. Additionally, the spectral reshaping can cause a decrease of the output bandwidth, e.g. by clipping the blue end of the spectrum. A more detailed description of the amplification process is given in [10].

Furthermore, a significant limitation of the overall bandwidth can be given by the mirrors, especially 45° steering mirrors in p-polarization. This restriction can be relaxed by using either s-polarization or specially designed chirped mirrors.

2 Setup

A schematic of the system is shown in Fig. 3. The mirror-dispersion-controlled Ti:sapphire oscillator (FemtoSource Pro; FemtoLasers GmbH) pumped by a diode-pumped frequency-doubled Nd:YVO₄ laser (Millenia; Spectra-Physics, Inc.) delivers sub-10 fs pulses of a few nJ energy at 75 MHz repetition rate. Owing to the use of broadband chirped mirrors instead of prisms for dispersion control, the bandwidth of the output extends over a range of ≈ 140 nm. Due to this broad bandwidth, the material dispersion of a 10-cm-long SF57 glass block and the Faraday isolator at the entrance of the amplifier is sufficient to stretch the pulses up to ≈ 20 ps. This grating-less stretching technique provides high efficiency and no need for alignment.

After temporal shaping, the pulse train is injected into a multipass amplifier arrangement. The amplifier consists of two curved mirrors, two retroreflectors and a 3.5-mm-long Brewster-cut Ti:sapphire crystal. The highly doped Ti:sapphire crystal ($\alpha = 3.5 \text{ cm}^{-1}$) is placed in a vacuum

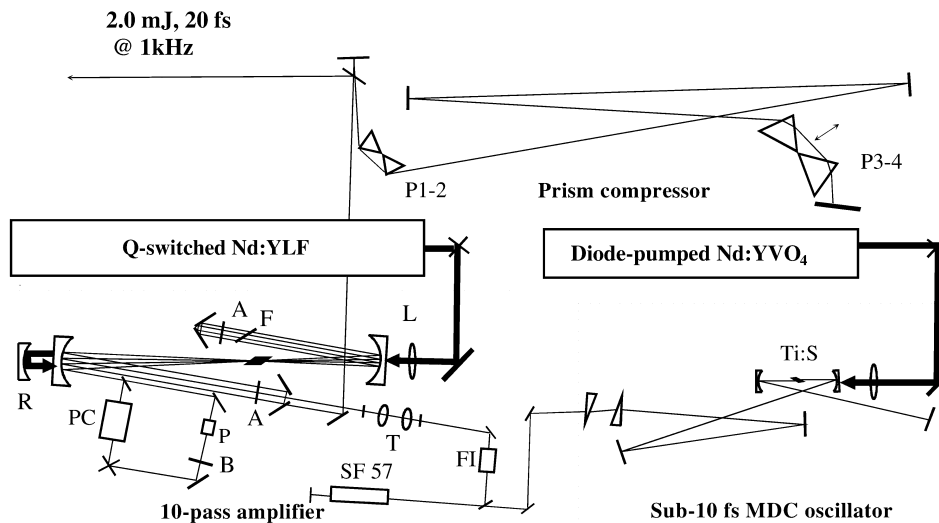


Fig. 3. Schematic of the laser system. SF57, heavy flint glass; F, shaping filter; FI, Faraday isolator; A, apertures; PC, Pockels cell; B, Berek polarization compensator; P, polarizer; T, demagnifying telescope; L, lens for pump beam; R, reflector for residual pump beam; P1-4, fused-silica prisms, numbered 1–4

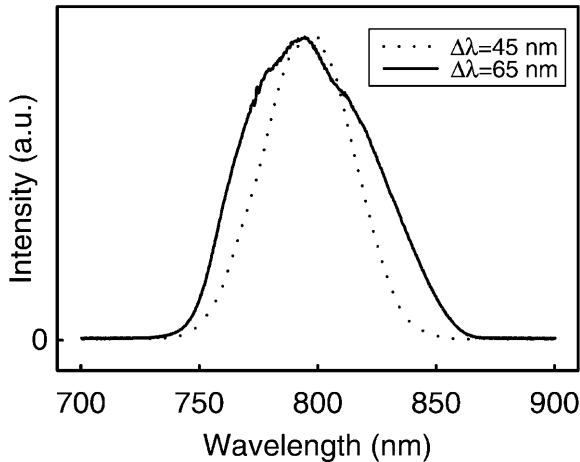


Fig. 4. Effect of the specially designed spectral shaping filter. Measured amplified spectrum without (*dotted*) and with (*solid*) filter

chamber and is thermo-electrically cooled down to $-15\text{ }^{\circ}\text{C}$ to reduce the effect of thermal lensing. One of the retro-reflectors is made up of two chirped mirrors specially designed for providing third- and fourth-order dispersion control to compensate for the higher-order-dispersion of the prism compressor and all the material in the amplifier.

During the first four passes, the pulses go through a dielectric multilayer filter providing the total transmission curve shown in Fig. 2a. Thus gain narrowing is partially compensated for, increasing the amplified bandwidth by $\approx 50\%$ (Fig. 4). This spectral reshaping is at nearly no cost to overall power gain because of the strong saturation of the amplifier. In contrast with etalons or birefringent plates previously used for amplitude shaping, dielectric filters allow almost arbitrary transmission characteristics.

After four passes through the crystal, a single pulse is selected out of the pulse train with a Pockels cell. In this way both the ASE background and the susceptibility to lasing are suppressed. The measured ASE energy contained in the 10 ns Pockels cell time window is $2.7\text{ }\mu\text{J}$, yielding a pulse-to-pedestal intensity contrast of $\approx 10^9$.

The selected single pulse is reinjected and amplified in another six passes, where it picks up an additional $1\text{-}\mu\text{s}$ -long ASE background of 210 nJ energy. Before the last two passes, the pulse is coupled-out once again and reinjected after a reduction of the beam diameter by a factor of two. This allows optimization of the mode overlap of pump and seed beam, thus maximizing the energy extraction in the last two passes. In addition, nonlinear effects in the gain medium are reduced, keeping the B-integral low (of the order of unity). Pumping this optimized amplifier with 10.5 mJ from a lamp-pumped Q-switched frequency-doubled Nd:YLF laser results in a pulse energy of 2 mJ.

The amplified pulses are compressed with a prism compressor consisting of two pairs of Brewster-angled fused-silica prisms separated by 6 m. After passage through the prism compressor, the pulse duration is less than 20 fs and the beam diameter is 25 mm. The good energy extraction efficiency in the amplifier and the high throughput of the prism compressor ($\approx 90\%$) results in an overall efficiency (from nanosecond pump pulses into femtosecond amplified pulses) of 17%.

3 Characterization

Using these pulses for experiments, such as studying the interaction of intense laser fields with matter, calls for a precise knowledge of the pulse characteristics. To this end, we have characterized the temporal evolution with a SHG-FROG [11, 12] apparatus and, over an enhanced dynamic range, with a third-order autocorrelator, the beam quality and focusability with a CCD camera, and the spectrum with a grating spectrograph.

A typical SHG-FROG trace is shown in Fig. 5. The retrieved pulses have a duration of 17.5 fs and a bandwidth of 65 nm. The retrieved amplitude spectrum fits well to the one measured; and the spectral phase is reasonably flat over the whole spectral range, indicating a proper compensation of phase errors.

Figure 6 shows a high-dynamic-range autocorrelation based on third-harmonic generation directly on a glass surface [13]. It indicates a drop of the intensity of nearly three orders of magnitude within 100 fs at the leading edge and four orders of magnitude within less than 350 fs. Previous experiments have shown that, if required for certain experimental applications, the leading pulse edge can be steepened up by application of positive TOD [13].

We have also performed an M^2 measurement, yielding a value of approximately 1.5 in both planes. For this purpose we focused the beam with $f/100$ optics and recorded the beam diameters (x - and y -plane) at several positions in front and be-

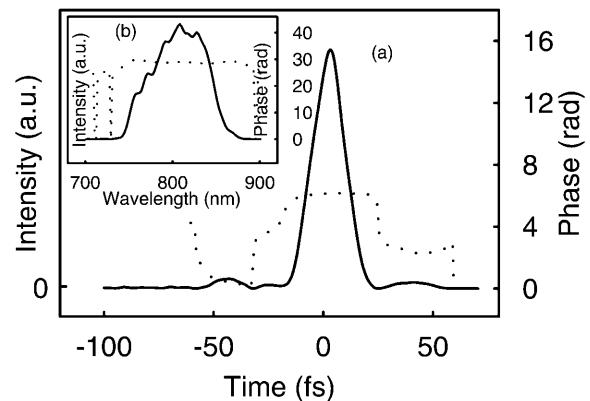


Fig. 5a,b. Measured SHG-FROG. **a** Temporal intensity (*solid*) and phase (*dotted*). **b** Spectral intensity and phase

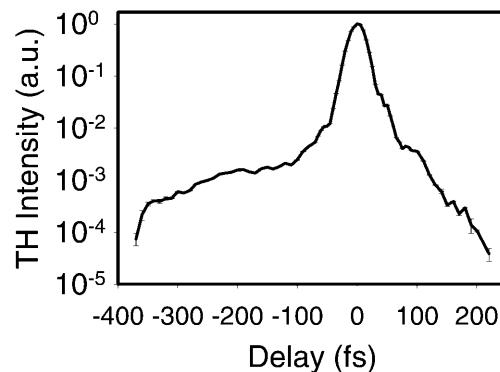


Fig. 6. Measured THG-autocorrelation



Fig. 7. Focal spot of 3.5 μm diameter

hind a beam waist with a CCD camera. For evaluation of M^2 , its defining equation [9]

$$w(z) = w_0 \sqrt{1 + \left[M^2 \left(\frac{z}{z_R} \right) \right]^2} \quad (6)$$

has been fitted to the measured data. Here w is the measured beam radius, w_0 the radius at the beam waist, z the longitudinal coordinate and z_R the rayleigh range given by $w_0^2 \pi / \lambda$.

By utilizing a diamond-turned off-axis parabolic mirror of 33 mm focal length ($f/1.3$ optics), some 70% of the pulse energy can be concentrated within a spot of a $1/e^2$ diameter of 3.5 μm , which was imaged with a $100\times$ microscope objective onto a CCD camera. This results in a peak intensity of approximately $6 \times 10^{17} \text{ W/cm}^2$. The contour plot in Fig. 7 depicts isointensity lines at the levels of $I_p/8$, where I_p is the peak intensity in the focal plane. The distortions surrounding the central spot originate from the mirror itself, since the surface of a diamond-turned mirror exhibits grooves acting as

a grating. In this manner some 10% of the energy is diffracted into higher-order modes.

4 Conclusions

We have demonstrated the kHz-rate generation of femtosecond pulses at the 0.1 TW level from a single-stage amplifier for the first time. A detailed characterization yields sub-20 fs pulse duration, a drop in the intensity by more than four orders of magnitude at 350 fs prior to the peak of the pulse, and a focused peak intensity close to 10^{18} W/cm^2 . These characteristics open the way to performing high-field experiments at a high repetition rate with a compact (occupied table space: $\approx 2.5 \text{ m}^2$) user-friendly system. Furthermore, this source has the potential to be scaled up to output energies of $\approx 10 \text{ mJ}$, implementing a second amplifier stage.

Acknowledgements. This work was supported by the Austrian Science Fund, Grant Y44-PHY. The generous donation of several key components of the presented system by Femtolasers GmbH is gratefully acknowledged.

References

1. See e.g. special issue on Ultrafast Optics IEEE J. Sel. Top. Quantum Electron. 4, (1998)
2. C. Le Blanc, E. Baubeau, F. Salin, J.A. Squier, C.P.J. Barty, Ch. Spielmann: IEEE J. Sel. Top. Quantum Electron. 4, 407 (1998)
3. S. Backus, C.G. Durfee III, M.M. Murnane, H.C. Kapteyn: Proceedings Ultrafast Phenomena XI, p. 41 (1998)
4. Y. Nabekawa, Y. Kuramoto, T. Togashi, T. Sekikawa, S. Watanabe: Opt. Lett. 23, 1384 (1998)
5. E.T.J. Nibbering, O. Dühr, G. Korn: Opt. Lett. 22, 1335 (1997)
6. V. Bagnoud, F. Salin: Ultrafast Optics 99 Program, p. 16 (1999)
7. S. Sartania, Z. Cheng, M. Lenzner, G. Tempea, Ch. Spielmann, F. Krausz, K. Ferencz: Opt. Lett. 22, 1562 (1997)
8. J. Diels, W. Rudolph: *Ultrashort Laser Puls Phenomena* (Academic Press, Inc., San Diego, California, 1996)
9. A.E. Siegman: *Lasers* (University Science Books, Mill Valley, California, 1986)
10. C. Le Blanc, P. Curley, F. Salin: Opt. Commun. 131, 391 (1996)
11. R. Trebino, D.J. Kane: J. Opt. Soc. Am. A. 10, 1101 (1993)
12. K.W. De Long, R. Trebino, J. Hunter, W.E. White: J. Opt. Soc. Am. B. 11, 2206 (1994)
13. M. Hentschel, S. Uemura, Z. Cheng, S. Sartania, G. Tempea, Ch. Spielmann, F. Krausz: Appl. Phys. B 68, 145 (1999)